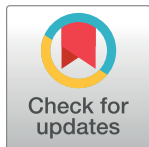# PLOS ONE

RESEARCH ARTICLE

Regeneration of a full-thickness defect in rotator cuff tendon with umbilical cord-derived mesenchymal stem cells in a rat model

Ji-Hye Yea[1,2], InJa Kim[2], Gayoung Sym[2], Jin-Kyung Park[2], Ah-Young Lee[2], Byeong Chan Cho[3], Tae Soo Bae[3], Byoung Jae Kim[4], Chris Hyunchul Jo[1,2]*

1 Department of Translational Medicine, Seoul National University College of Medicine, Seoul, Korea, 2 Department of Orthopedic Surgery, SMG-SNU Boramae Medical Center, Seoul National University College of Medicine, Seoul, Korea, 3 Department of Biomedical Engineering, Collage of Science and Engineering, Jungwon University, Goesan-gun, Chungcheongbuk-do, Korea, 4 Department of Obstetrics & Gynecology, SMG-SNU Boramae Medical Center, Seoul National University College of Medicine, Seoul, Korea

* chrisjo@snu.ac.kr

Abstract

Although rotator cuff disease is a common cause of shoulder pain, there is still no treatment method that could halt or reveres its development and progression. The purpose of this study was to investigate the efficacy of umbilical cord-derived mesenchymal stem cells (UC MSCs) on the regeneration of a full-thickness rotator cuff defect (FTD) in a rat model. We injected either UC MSCs or saline to the FTD and investigated macroscopic, histological and biomechanical results and cell trafficking. Treatment with UC MSCs improved macroscopic appearance in terms of tendon thickness at two weeks, and inflammation, defect size, swelling/redness and connection surrounding tissue and slidability at four weeks compared to the saline group. Histologically, UC MSCs induced the tendon matrix formation recovering collagen organization, nuclear aspect ratio and orientation angle of fibroblast as well as suppressing cartilage-related glycosaminoglycan compared to saline group at four weeks. The UC MSCs group also improved ultimate failure load by 25.0% and 19.0% and ultimate stress by 27.3% and 26.8% at two and four weeks compared to saline group. UC MSCs labeled with PKH26 exhibited 5.3% survival at four weeks compared to three hours after injection. This study demonstrated that UC MSCs regenerated the FTD with tendon tissue similar properties to the normal tendon in terms of macroscopic, histological and biomechanical characteristics in a rat model.

Introduction

Shoulder pain results in over 4.5 million physician visits, and rotator cuff disease is the most common cause of shoulder pain accounting up to 70% of cases with approximately 300,000 operations each year in the United States [1, 2]. The spontaneous healing potential of tendon is

very limited [3]. Once injured or diseased, tendinopathy typically progresses without recovery.
Current conservative treatments for rotator cuff disease include rest, non-steroidal anti-
inflammatory drugs, physical therapy and various kinds of injections [4, 5]. However, the suc-
cess rate for conservative treatment varies widely from less than 50% to greater than 90% [6].
A considerable number of patients, 41%, showed persistent symptoms after 12 months of treat-
ment [7]. These results may be attributed to the fact that those symptomatic treatments do not
address the fundamental etiology of rotator cuff disease, most importantly tendon degenera-
tion [8]. As tenocytes in degenerative tendon do not participate in the regeneration process
[9], it would be momentous to investigate new biological strategies such as application of vari-
ous cells, growth factors and cytokines to more adequately treat tendon degeneration [10].

A promising therapeutic strategy for recovering damaged tissues is the use of mesenchymal
stem cells (MSCs) which may be derived from various tissues such as bone marrow (BM), adi-
pose tissue (AD), muscle tissue (MT) and umbilical cord blood (UCB) [11]. Recently, a few stud-
ies have shown that MSCs were effective in regenerating rotator cuff tendon [12, 13]. BM MSCs
improved early collagen organization and collagen fiber coherence, and they enhanced the ten-
sile strength of repaired rotator cuff tendon in an athymic rat model [12]. AD MSCs decreased
inflammatory cells and improved collagen fiber arrangement and organization as well as
enhancing the tensile strength of rotator cuff tendon in a rat model of collagenase-induced rota-
tor cuff injury [13]. However, use of these MSCs has been criticized for several disadvantages
including invasive techniques for harvesting [9], low collection efficiency [14], decreased quality
with the age and morbidities of donors, and concerns of heterotopic ossification [15]. Thus, it
would be worthwhile to find alternate cell sources to overcome these drawbacks.

Umbilical cord derived MSCs (UC MSCs) are fetal MSCs isolated from umbilical cords tis-
sue which are usually discarded as medical waste after delivery, and thus can be obtained non-
invasively at collection and can be supplied at relatively low cost [14]. UC MSCs are reported
to be more proliferative and have higher self-renewal potential than other adult MSCs [16].
UC MSCs are able to differentiate towards the myogenic lineage and contributed to the muscle
regenerative process of tibialis anterior muscle injury in a rat model [17]. UC MSCs were also
able to differentiate endothelial cells and contributed to the muscle regenerative process of a
hindlimb ischemia injury in a mouse model [18]. In addition, the conditioned medium of UC
MSCs increased dermal fibroblast proliferation and migration and the medium accelerated
wound healing with fewer scars of full-thickness skin excisional wounds injury in a C57BL6
mouse [19]. Human umbilical cord perivascular cells facilitated tendon regeneration through
changes in collagen organization, cell shape and orientation, and increase in mechanical prop-
erties in an athymic rat model of collagenase-induced Achilles tendon injury simulating a
chronic tendon inflammation [20]. Although few studies using UCB MSCs derived from
umbilical cord blood have been reported for tendon healing [21, 22], but there is yet no report
on the efficacy of UC MSCs for rotator cuff regeneration despite these potentials of UC MSCs
for musculoskeletal tissue regeneration.

Hence, the purpose of this study was to investigate the efficacy of UC MSCs on the regener-
ation of a full-thickness rotator cuff defect (FTD) in a rat model. We hypothesized that UC
MSCs would regenerate the FTD with tendon tissue similar properties to the normal tendon
in terms of macroscopic, histological and biomechanical characteristics.

Materials and methods

Study design

This study was approved by the Seoul Metropolitan Government Seoul National University
Boramae Medical Center Institutional Animal Care and Use Committee and the Seoul

Metropolitan Government Seoul National University Boramae Medical Center Institutional Review Board (IACUC_2017_0021 and IRB No. 16-2015-115). This study was carried out in strict accordance with the recommendations in the guide for the IACUC and IRB. All surgery was performed under anesthesia, and all efforts were made to minimize suffering. Eighty-four adult male Sprague-Dawley rats (12 weeks old, 340~360g) were divided into one of three groups and treated accordingly; 1) the control group (n = 24); 2) the saline group (n = 24); 3) the UC MSCs group (n = 36). Rats from each group were sacrificed at three hours, two and four weeks after surgery. The supraspinatus tendon tissue (SST) was harvested and used for macroscopic (n = 4; two and four weeks respectively) and histological evaluation (n = 4; the tissue used for macroscopic evaluation is used for histology analysis), biomechanical evaluation (n = 8; two and four weeks respectively), and cell trafficking evaluation (n = 4; three hours, two and four weeks respectively).

UC MSC isolation and culture

Human umbilical cords were obtained from healthy full-term deliveries by cesarean section after informed consent, and UC MSCs were isolated and cultured using minimal cube explant method.

UCs were washed 2–3 times with Dulbecco's Phosphate-Buffered Saline (DPBS; Welgene, Daegu, Korea) to remove blood products and then measured for length and weight, and then cut into minimal cube explants of 2–4 mm by surgical scissors. The cube explants (1 g) were aligned at regular intervals in 15-cm culture dishes and allowed to firmly attach to the bottom of the dish for 60 mins in a 5% CO_2 incubator with humidified air at 37 °C. Then, the culture medium consisting of low-glucose Dulbecco's modified Eagle medium (LG-DMEM; Hyclone, Logan, USA) supplemented with 10% fetal bovine serum (FBS; Hyclone) and antibiotic-antimycotic solution (100 U/ml penicillin, 100 μg/ml streptomycin, and 0.25 μg/ml amphotericin B; Welgene) was gently poured into the dishes. The medium was replaced twice a week. Non-adherent cells were removed by medium changes. When cells reached 60–80% confluence, they were detached by incubation for 3 min with trypsin-EDTA (0.05% trypsin, 0.53 mM EDTA; Welgene). The tissues were removed through a 100 μm cell strainer (SPL Life Sciences, Pocheon, Korea) and the cells were centrifuged at 500 g for 5 min at 20 °C and then replated at a density of 3×10^3 cells/cm^2.

Surface phenotypic characterization by flow cytometry was performed as previously reported [23]. Briefly, a total of six antibodies were used: CD34-PE, CD45-PE, CD73-PE, CD90-FITC, CD105-FITC and HLA-DR-FITC (BD Biosciences, San Jose, CA, USA). Once the cells had been detached, aliquots of 5×10^5 cells were washed twice with DPBS, centrifuged, washed in ice cold DPBS supplemented with 2% fetal bovine serum (FCM buffer) and fixed in 1% paraformaldehyde in FCM buffer, followed by incubation with fluorescein isothiocyanate (FITC) or phycoerythrin (PE)- conjugated antibodies for 30 min on 4 °C in a dark room. Data were obtained by analyzing 10,000 events on a Flow Cytometer FC500 (Beckman Coulter, Brea, CA, USA) with CXP Cytometer 2.3 software (Beckman Coulter, Brea, CA, USA). All analyses were standardized against isotype controls [24].

UC MSCs at passage 10 were used for all experiments and characterization including morphology, growth kinetics, CFU-F, flow-cytometric and trilineage differentiation of cells was performed as previously reported [23].

Surgical procedures

Anesthesia was induced using zoletil and rompun (30mg/kg + 10mg/kg). The left shoulder was operated on in all cases. A 2cm skin incision was made directly over the anterolateral
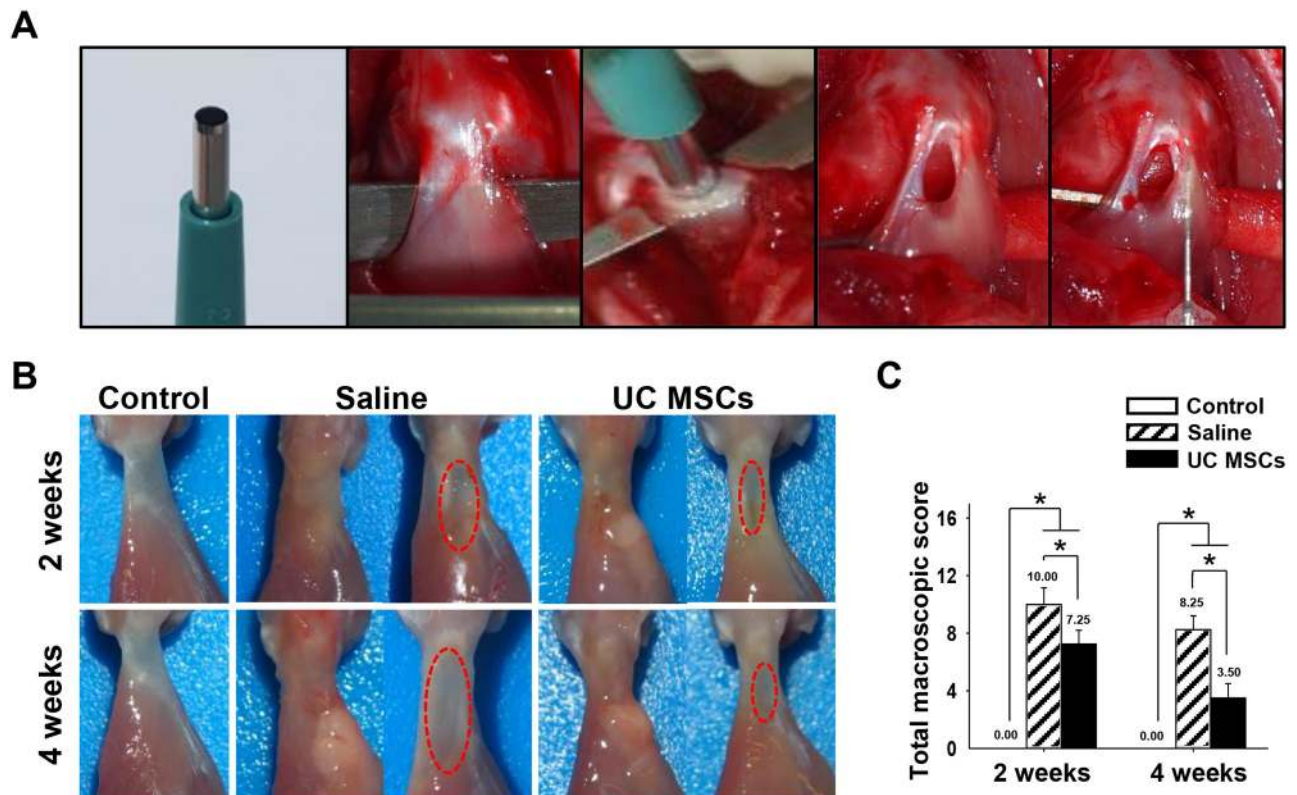
Fig 1. Procedure of surgery, macroscopic images, and quantification of macroscopic appearance of regenerated tendons at two and four weeks.
(A): Surgical procedure of FTD and intratendinous injection of saline or UC MSCs. (B): Macroscopic appearance of the tendon (Left side image: Supraspinatus tendon immediately after harvest; Right side image: the tendon removing the loose connective tissue surrounding the injury site to observe the original defect shape). (C): The total macroscopic score. Bar charts present mean ± standard deviation; Statistically significant at $p < .05$. Abbreviations: UC MSCs, umbilical cord derived mesenchymal stem cells.

https://doi.org/10.1371/journal.pone.0235239.g001

border of the acromion. After the SST was exposed by detaching trapezius and deltoid muscle from the acromion, a round FTD with a diameter of 2mm in the middle of the SST was created 1mm from the insertion using a Biopsy Punch (BP-20F, Kai Medical Europe GmbH, Bremen, Germany). This defect size was approximately 50% of the tendon width, correlating to a large but not a massive tear according to the method previously described [25, 26]. Ten microliter of saline, UC MSCs (1×10^6 cells) and PKH26 labeled UC MSCs (1×10^6 cells) were intratendinously injected adjacent to both sides of the defect in two divided doses via 30 G needle (Fig 1A). After injection, the deltoid and trapezius muscles were sutured with a 4–0 Vicryl suture (W9074, Ethicon, Cincinnati, OH, USA) and then skin was also sutured with a black silk (SK439, AILee, Busa, Korea). In the control group, the SST was exposed, but no further surgical procedure was performed (the sham control). After surgery, animals were allowed free cage activity. The condition of animals was checked by veterinarians and zookeepers [24].

Macroscopic evaluation

At two and four weeks after injection, the rats were sacrificed in a carbon dioxide chamber. The SST of the rats were harvested with humerus head without removing the muscle. For macroscopic evaluation of tendon regeneration, we used a modified semi-quantitative system of Stoll *et al.* [27] (see the S1 Table). The total macroscopic score could vary between 0 (normal tendon) and 15 (most severely injured) [24].

Histological evaluation

After the macroscopic evaluation, the harvested tissues were immediately fixed in 4% (w/v) paraformaldehyde (PFA; Merck, Darmstadt, Germany) for 24 hours, and underwent decalcification in 10% ethylendiaminetetracetic acid (EDTA; Sigma-Aldrich, St Louis, MO, USA) for two days. After decalcification, the tissues were dehydrated through an increasing ethanol gradient, defatted in chloroform, and embedded in paraffin blocks. The tissue was carefully trimmed to the appropriate middle site of tendon and cut into 4-μm thick serial sections.

A randomly selected slide was stained with hematoxylin and eosin (H&E) and analyzed by light microscopy (U-TVO 63XC; Olympus Corp., Tokyo, Japan). For the evaluation of tendinopathy, each slide was evaluated using the semi-quantitative grading scale as previously described [28]. The 7 parameters of the system include; fiber structure, fiber arrangement, rounding of the nuclei, variations in cellularity, vascularity, stainability, and hyalinization. Each parameter in the grading scales varies from 0 to 3. The total degeneration score for a given slide varied between 0 (normal tendon) and 21 (most severely degenerated).

Integration of structure were evaluated using a 0–3 grading scale: 0 (normal), 1 (slightly abnormal), 2 (moderately abnormal) and 3 (maximally abnormal) [29].

Infiltration of inflammatory cells were evaluated using a 0–3 grading scale: 0 (normal; <10% area infiltrated by inflamed cells), 1 (slightly abnormal; 10%~20% area infiltrated by inflamed cells), 2 (moderately abnormal; 20~30% area infiltrated by inflamed cells) and 3 (maximally abnormal; >30% <10% area infiltrated by inflamed cells) [29].

We also evaluated the occurrence of heterotopic ossification when separated, clustered and bar-shaped foci were found in the whole tendon structure [30].

In normal tendon, the few fibroblasts with flattened nuclei are typically aligned parallel to the tensile axis. After injury, the morphometric changes of fibroblast nuclei were evaluated as previously described by Fernandez-Sarmiento using H&E stained slides [31]. Fibroblast density (number of nuclei per mm^2), nuclear aspect ratio (the ratio of the minor diameter to the maximal diameter), and nuclear orientation angle (between the major axis of the nuclear angle and the axis of collagen fibers) were evaluated. Five regions of interest (ROI) were measured and the average was used finally.

Slides were stained with picrosirius red (PSR) for analysis of collagen fiber organization and coherency using circularly polarized light microscopy at x200 magnification. Collagen organization was measured as intense white areas of brightly diffracted light on gray scale (black, 0; white, 255) using ImageJ software with installed NII plugin (National Institutes of Health, MD, USA). Higher gray scale indicated more organized and mature collagen [32]. The coherence of the collagen fibers is a measure of the extent of fiber alignment in the major axis of alignment. The coherence was quantified using the Orientation J plug-in for image J and then multiplied by 100 to obtain the final coherence value [12]. Five ROIs were measured and the mean value was used.

For evaluation of cartilage formation, slides stained with Safranin-O/fast green (Saf-O) were used and observed via light microscopy at x 200 magnification. The glycosaminoglycan (GAG)-rich area was measured using image J [15, 24].

Biomechanical evaluation

For biomechanical testing, we harvested supraspinatus tendon with humerus head and carefully removed the muscles to leave only the tendon. The harvested tissues were wrapped in saline-soaked gauze and kept at -80 ˚C. Before testing, the tissues were thawed with saline wet gauze at room temperature for 24 hours and the tissues were kept moist with saline during all tests. The distal part of humerus bone was vertically embedded in an aluminum tube full of

polymethylmethacrylate (PMMA) in the custom-designed lower jig of a testing system. The proximal end of tendon was compressed with sandpaper, gauge, and rubber to prevent slippage and to reduce damage of specimens. The complex was clamped vertically in the custom-designed upper jig. Testing was performed with shoulders at 90˚ of abduction with a material testing system (H5K5, Tinus Olsen, England, UK) [33, 34]. All specimens were loaded to failure in tension at a constant rate of 0.1 mm/s. Slippage of the tendon was inspected visually. The cross-sectional area of supraspinatus tendon was measured at the center of defect region. The area was calculated with the formula (Area = width x thickness x π). From the load-displacement curve recorded during tests, the ultimate failure load, the stiffness and ultimate stress was calculated [24, 35, 36].

UC MSCs trafficking

UC MSCs were labeled with fluorescent PKH26 (Sigma-Aldrich, St Louis, MO, USA) according to the manufacturer's protocol that is known to have an *in vivo* half-life of greater than 100 days and would be useful for *in vivo* cell trafficking [37]. When cells reached 60% to 80% confluence, they were detached by incubation for 5 minutes with 0.25% trypsin EDTA and washed three times with PBS After aspirating the supernatant in UC MSC containing tubes, the cells were resuspended gently in 1mL of the dilution buffer and mixed with an equal volume of the labeling solution containing $4x10^{-2}M$ PKH26 in the dilution buffer. Then, the cells were incubated at 5 min at room temperature and the reaction was terminated by addition 2 mL of FBS. The suspension was centrifuged at 400xg for 5 min and the cells were washed three times with PBS. After labeling, the cells were counted by hemocytometer, and confirmation of red fluorescence was obtained by fluorescence microscope (Leica DMI 4000B, Leica, Wetzlar, Germany) before injection [24].

At three hours, two and four weeks after injection, the tissue was harvested and used for evaluation. We harvested only supraspinatus tendon and the harvested tissues were immediately fixed in 4% (w/v) PFA for 24 hours. The tissues were treated with consecutive 10%, 15% and 20% sucrose/PBS solutions at 4˚C for 12h respectively. The tissues were embedded in O.C.T. compound (Tissue-Tek, Miles, USA) with subsequent freezing of the block at -80˚C. To evaluate the survival ability of the PKH 25 labeled UC MSCs, the specimens were sectioned (7 μm) with a freezing microtome (Leica CM3050S, Leica, Wetzlar, Germany) and carefully trimmed until we found middle side of tendon. The slides were mounted with Vectashield containing DAPI (Vector Laboratories Inc., Burlingame, CA). Five fields were randomly selected in the slide and high-powered images (x400) were obtained by fluorescence microscopy. The PKH26 positive cells coincident with 4′,6-diamidino-2-phenylindole (DAPI) were counted per area and the mean number were recorded by image J [38].

Statistical analysis

All data are shown as mean ± SD. The data was analyzed with one-way analysis of variance (ANOVA) with post hoc analysis using Bonferroni multiple comparison test. All statistical analyses were performed with SPSS software version 23 (IBM). Differences of $p < .05$ were considered statistically significant.

Results

Macroscopic evaluation

For macroscopic scoring, tendon thickness score was significantly less in the UC MSCs group in comparison with that in the saline group ant the total macroscopic score was significantly

lower in the UC MSCs group, 7.25 ± 0.96, than in the saline group, 10.00 ± 1.15 ($p = .005$) at two weeks. At four weeks, inflammation, defect size, swelling/redness and connection surrounding tissue and slidability score were significantly lower in the UC MSCs group than those in the saline group. The total macroscopic score was significantly lower in the UC MSCs group, 3.50 ± 1.00, than in the saline group, 8.25 ± 0.96 ($p < .001$) at four weeks (Fig 1B and 1C). Evaluation results of each parameters are shown in the S2 Table. Loose connective tissues surrounding the defect site was removed to observe the original defect (Fig 1B).

Histological evaluation

For the evaluation of tendinopathy, stainability score was significantly less in the UC MSCs group, 1.50 ± 0.58, in comparison with that in the saline group, 2.50 ± 0.58 (p = .045) at two weeks. However, the total degeneration score was not significantly different between the saline group, 16.50 ± 1.00, and the UC MSCs group, 15.50 ± 1.73 (p = .905) at two weeks (Fig 2A and 2B). At four weeks, fiber structure, fiber arrangement, rounding of the nuclei vascularity and hyalinization were significantly lower in the UC MSCs group, 1.25 ± 0.50, 1.00 ± 0.00, 1.00 ± 0.00, 1.25 ± 0.50 and 0.25 ± 0.50 than those in the saline group, 2.50 ± 0.58, 2.50 ± 0.58, 2.25 ± 0.50, 2.50 ± 0.58 and 1.75 ± 0.50 ($p = .009, < .001, .006, .025$ and $.002$ respectively). The total degeneration score was significantly less in the UC MSCs group, 7.00 ± 1.41, than in the saline group, 15.67 ± 2.08 ($p < .001$) (Fig 2A and 2B) at four weeks. The scores of structure integration and inflammation were not significantly different between the saline and UC MSCs groups at both two and four weeks (Fig 2A, 2C and 2D). There was no noticeable immune response against the UC MSCs. Heterotopic ossification was not observed in both groups at any time points.

Collagen organization score was not different between the groups at two weeks, but it became significantly higher in the UC MSCs group, 108.79 ± 12.36, than in the saline group, 78.67 ± 8.71 ($p = .005$) at four weeks (Fig 3A and 3B). Collagen fiber coherence score was not different between the groups at any time points (Fig 3A and 3C).

Fibroblast density was not significantly different between the groups at any time points (Fig 4A and 4B). Scores of nuclear aspect ratio and nuclear orientation angle were not significantly different between the two groups at two weeks. At four weeks, they became significantly lower in the UC MSCs group, 0.21 ± 0.02 and 6.49 ± 1.52, than in the saline group, 0.35 ± 0.07 and 21.61 ± 7.76 respectively ($p = .004$ and $.004$) at four weeks (Fig 4A, 4C and 4D).

Although cartilage-related GAG was formed in the saline group, 140 ± 162 mm^2, there was no significantly formation of cartilage-related GAG in UC MSCs group at two weeks. After four weeks, the GAG-stained area appeared in both the saline and the UC MSCs groups, and it was significantly less in the UC MSCs group, 281.01 ± 267.23 mm^2, than that in the saline group, 1,030.59 ± 206.12 mm^2, ($p = .001$) (Fig 4E and 4F).

Biomechanical evaluation

The cross-sectional area of the SST significantly increased in the saline and the UC MSCs groups, 3.12 ± 0.14 and 3.02 ± 0.24 mm^2, in comparison with that in the control group, 2.29 ± 0.22 mm^2, at two weeks ($p < .001$ and $< .001$) (Fig 5B). At four weeks, the cross-sectional area was significantly less in the UC MSCs group, 2.84 ± 0.23 mm^2, than that in the saline group, 3.28 ± 0.64 mm^2 ($p < .001$).

The ultimate failure load was significantly higher in the UC MSCs group, 17.58 ± 3.52 N and 22.68 ± 2.44 N, than those in the saline group, 13.18 ± 3.04 N and 18.37 ± 4.31 N, at two and four weeks, respectively ($p = .016$ and $.035$) (Fig 5C). The ultimate failure load in the UC
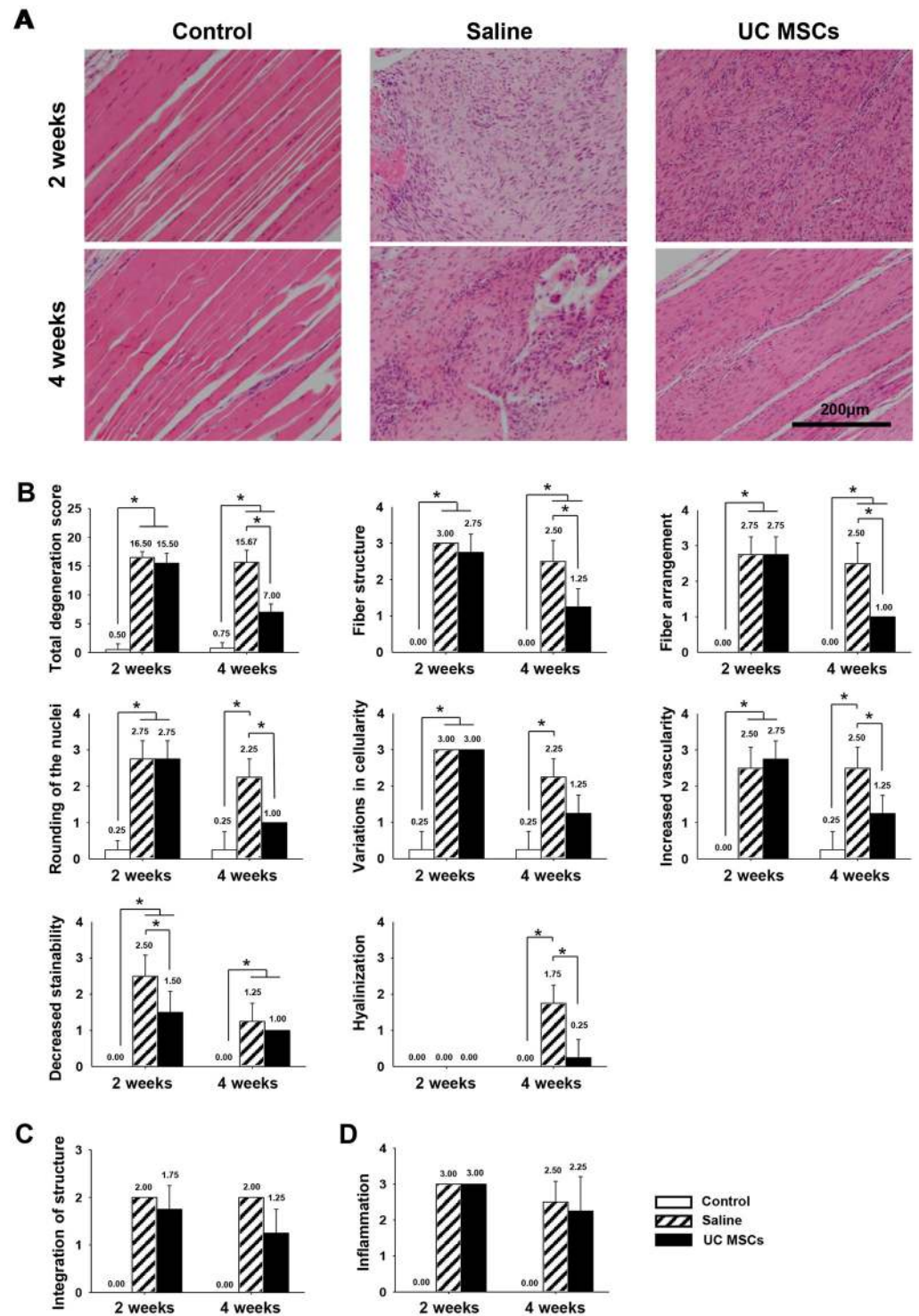
Fig 2. Representative histological images of general structure and quantification of the changes in regenerated tendon at two and four weeks. (A): H&E staining of tendon (magnification; X200). (B): the total degeneration score and detail parameters. (C): Integration of structure between the tendon defect and adjacent tendon. (D): Inflammation at the tendon defect. Bar charts present mean ± standard deviation; statistically significant at $p < .05$. Abbreviations: UC MSCs, umbilical cord derived mesenchymal; H&E, hematoxylin and eosin.
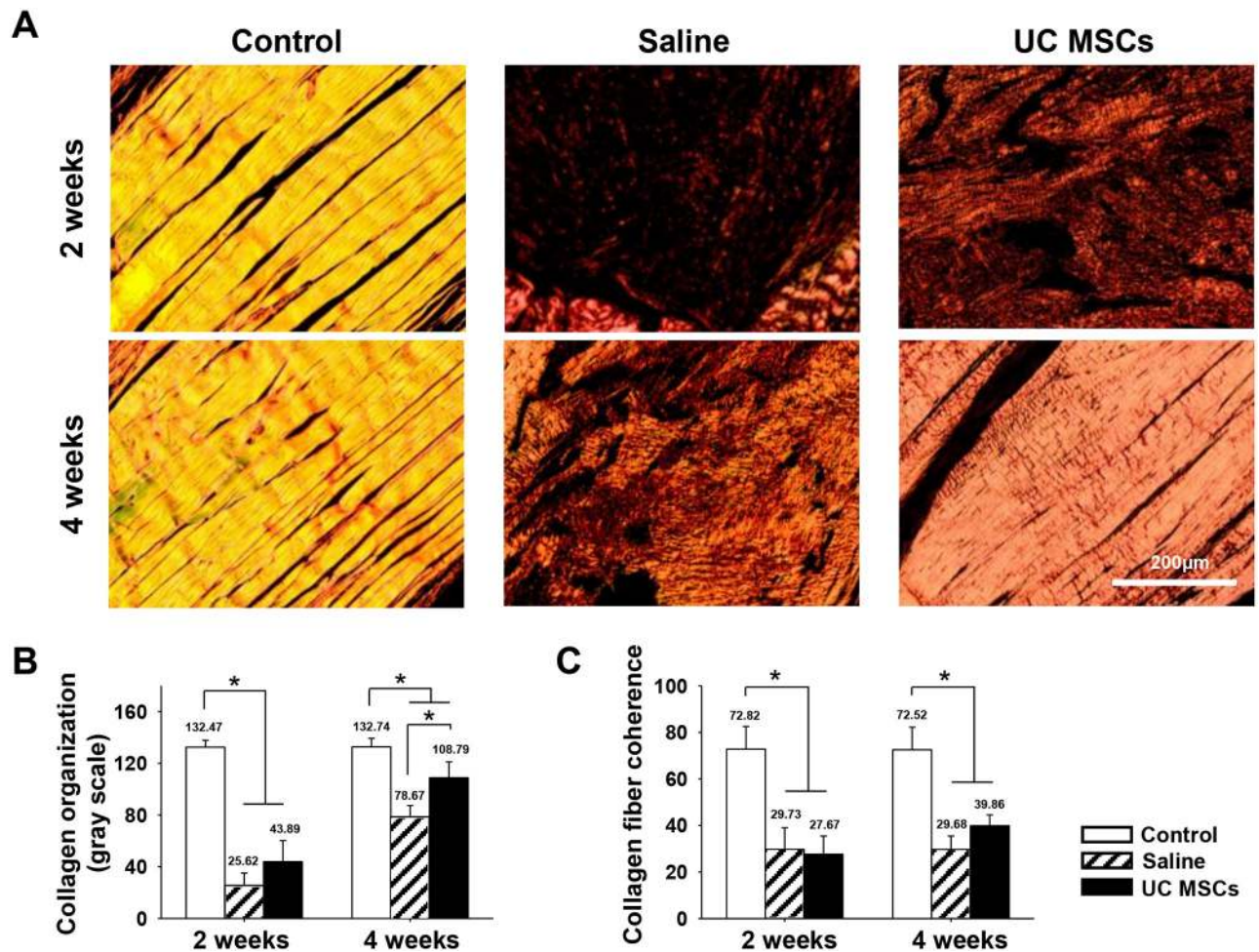
Fig 3. Representative histologic images of collagen matrix and quantification of the changes in regenerated tendon at two and four weeks. (A): PSR staining of the tendon (magnification; X200). (B): collagen organization of the tendon. (C): collagen fiber coherency of the tendon. Bar charts present mean ± standard deviation; statistically significant at $p < .05$. Abbreviations: UC MSCs, umbilical cord derived mesenchymal; PSR, picrosirius red.

MSC group at four weeks was comparable with that of the control group, 25.67 ± 2.17 N ($p = .159$).

The stiffness significantly improved in the UC MSCs group, 6.99 ± 1.05 N/mm than that in the saline group, 5.18 ± 0.90 N/mm at two weeks ($p = .018$) (Fig 5D). However, it was not different between the two groups at 4 weeks.

The ultimate stresses were significantly higher in the UC MSCs group, 5.77 ± 0.79 MPa and 7.97 ± 0.52 MPa, than those in the saline group, 4.20 ± 0.81 MPa and 5.84 ± 1.68 MPa, at two and four weeks, respectively ($p = .007$ and $p < .001$) (Fig 5E). However, the ultimate stress in both groups at four weeks was yet significantly less than that in the control group, 11.99 ± 1.89 MPa ($p < .001$ and $< .001$, respectively).

UC MSCs trafficking

Intratendinously injected UC MSCs disappeared over time, but they were retained in the tendon defect until 4 weeks after injection. At three hours after UC MSCs injection, the number of PKH 26 positive cells was 2135.36 ± 437.02 cells/mm^2 (Fig 6A and 6B). At two and four
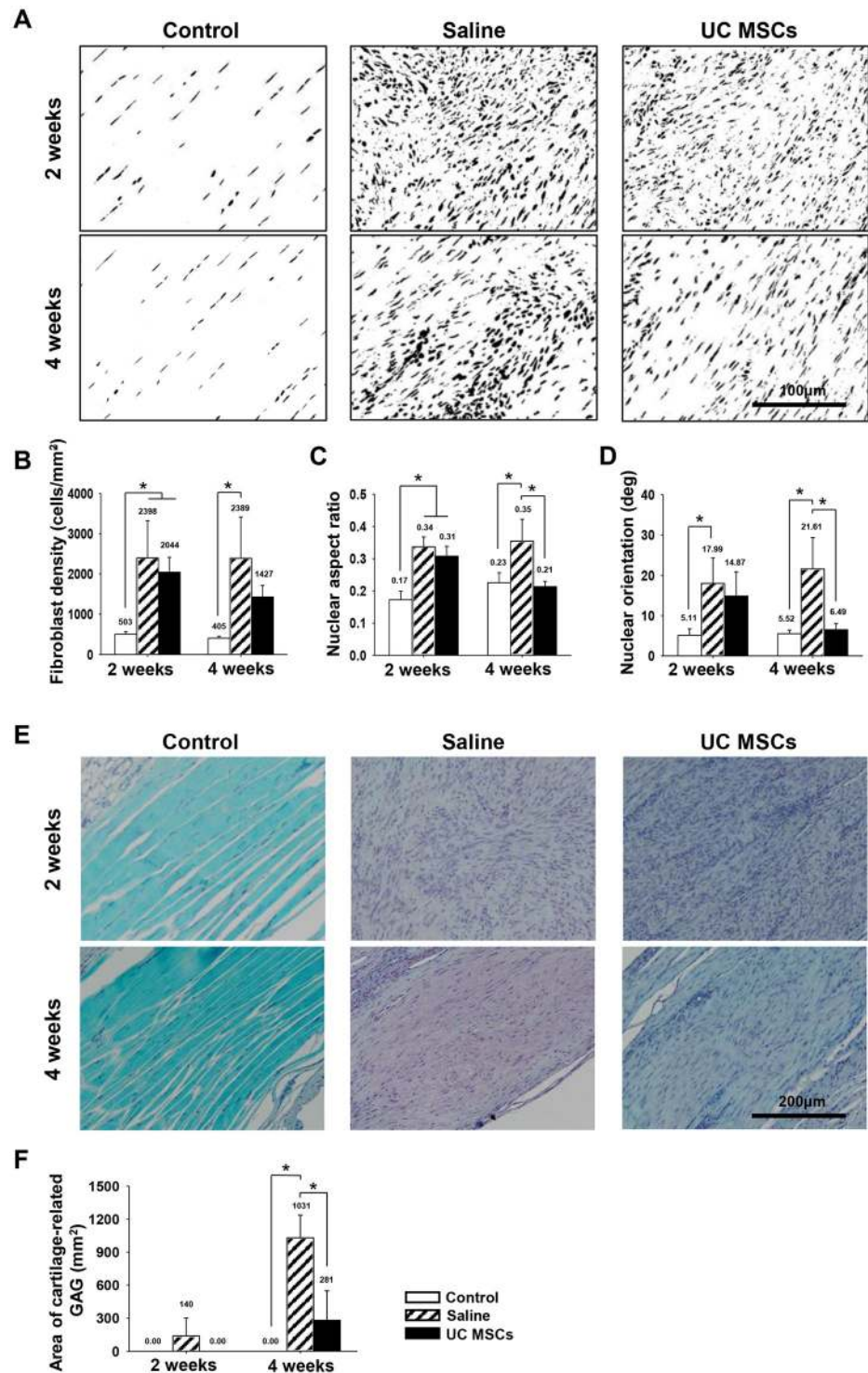
Fig 4. Representative histological images of nuclei morphology and cartilage formation of regenerated tendons and quantification of the changes at two and four weeks. (A): Nuclei morphology of fibroblasts at the tendon (magnification; X400) (B): Density of fibroblasts of the tendon. (C): Nuclear aspect ratio of fibroblasts of the tendon. (D): Nuclear angle of fibroblasts of the tendon. (E): Saf-O staining of the tendon (magnification; X200). (F): Area of cartilage-related GAG of the tendon. Bar charts present mean ± standard deviation; statistically significant at $p < .05$. Abbreviations: UC MSCs, umbilical cord derived mesenchymal; GAG, glycosaminoglycan; Saf-O, safranin-O.
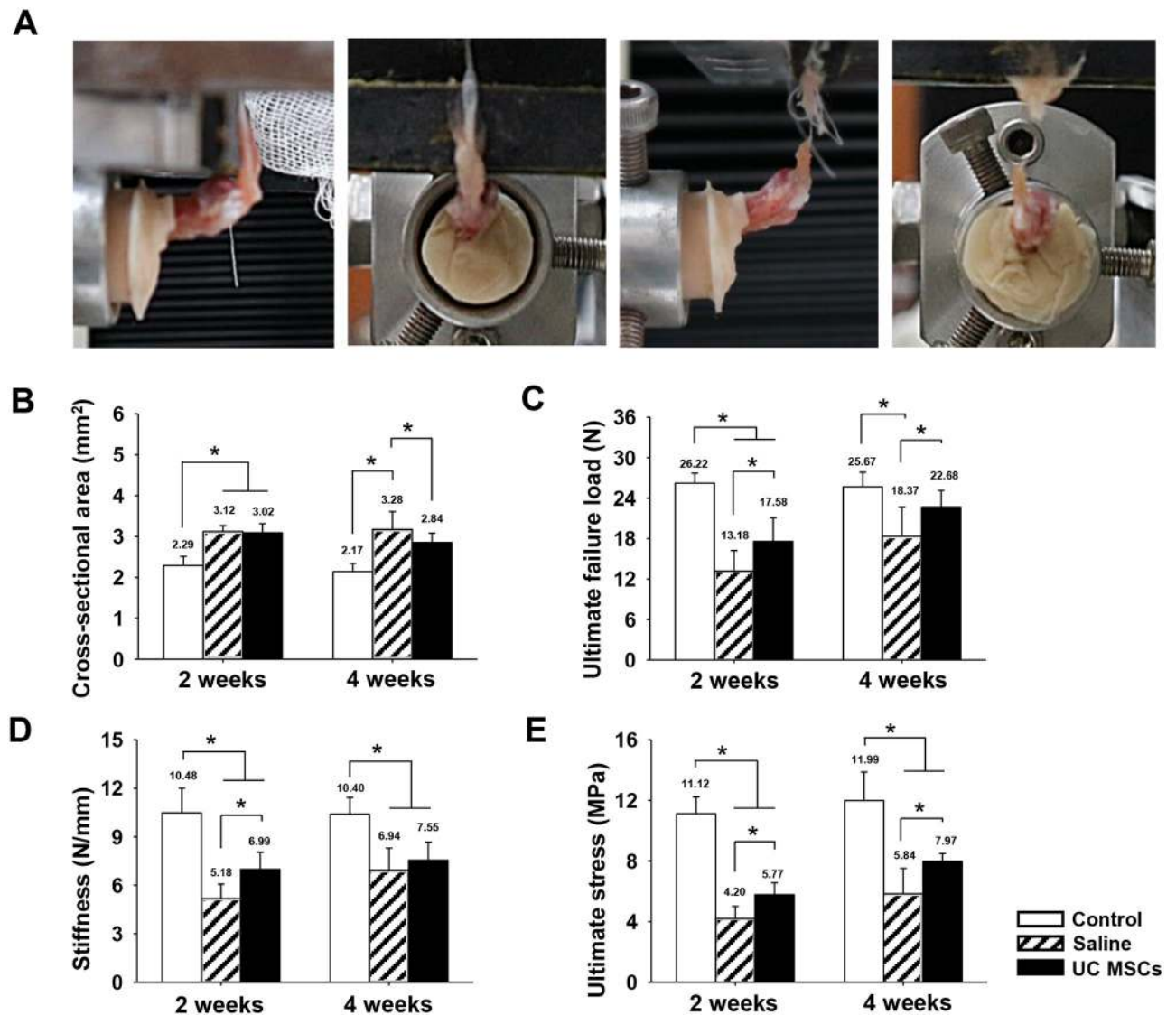
Fig 5. Biomechanical test procedure and quantification of biomechanical properties of regenerated tendons at two and four weeks. (A): an extracted specimen and procedure of biomechanical testing. (B): Cross-sectional area of the supraspinatus tendon at defect site. (C): ultimate failure load. (D): stiffness. (E): ultimate stress. Bar charts present mean ± standard deviation; statistically significant at $p < .05$. Abbreviations: UC MSCs, umbilical cord derived mesenchymal stem cells.

https://doi.org/10.1371/journal.pone.0235239.g005

weeks, it significantly decreased to 454.59 ± 137.40 cells/mm², 21.29% of that at three hours, and to 113.01 ± 21.39 cells/mm², 5.29% ($p < .001$ and $< .001$, respectively).

Discussion

The most important findings of this study are as follows; 1) the total macroscopic score significantly improved in the UC MSCs group compared to the saline group at two and four weeks through tendon thickness, inflammation, defect size, swelling/redness and connection surrounding tissue and slidability; 2) histologically, the total degeneration score significantly improved in terms of fiber structure, fiber arrangement, rounding of the nuclei, vascularity and hyalinization as well as the scores of nuclear aspect ratio, nuclear orientation angle, and
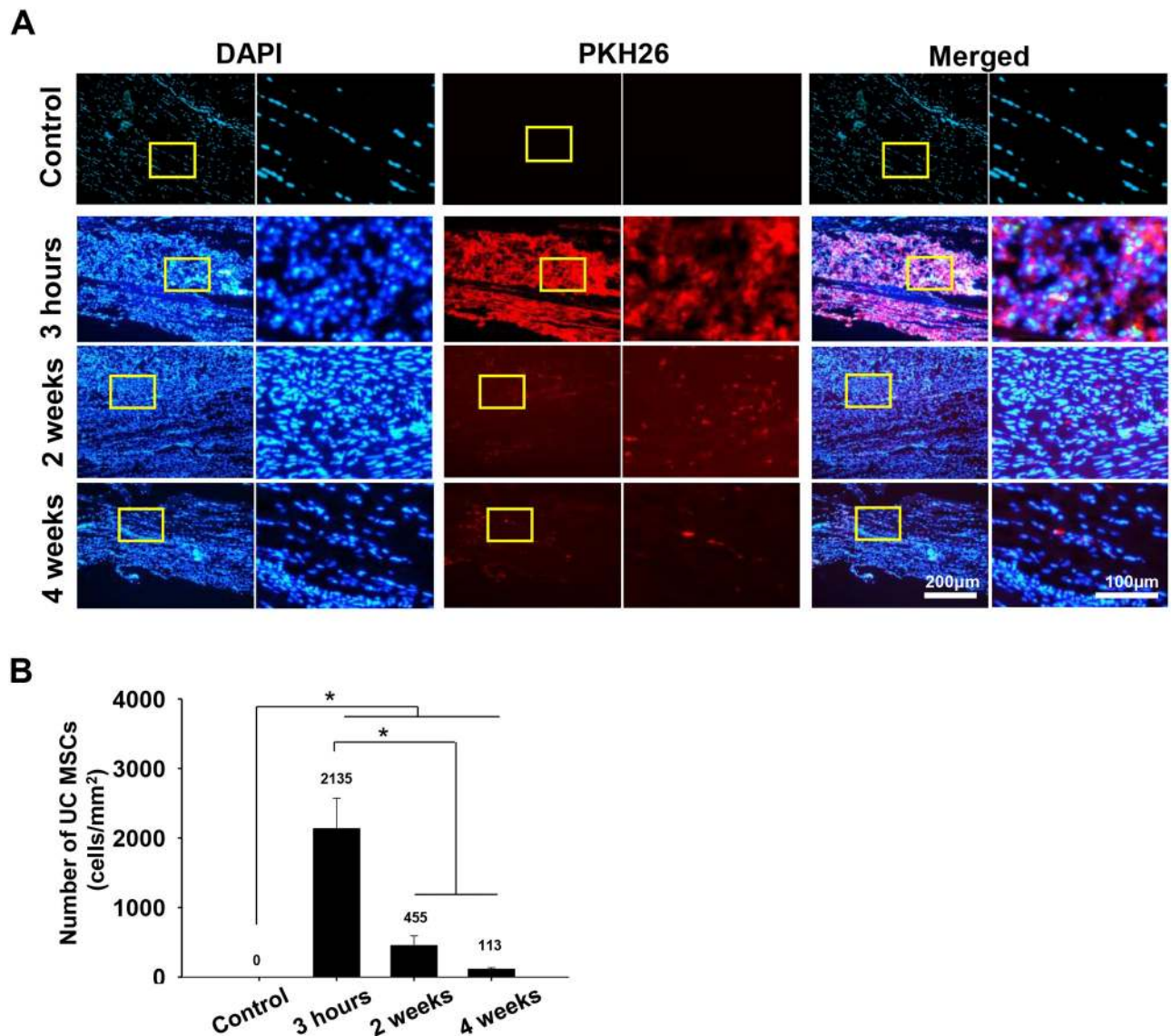
Fig 6. Representative fluorescent images of implanted PKH26 labeled UC MSCs within the SST and quantification of the injected cells at 3 hours and two and four weeks. (A): Implanted UC MSCs with DAPI and PKH26 dye of the tendon (magnification; X200 and X400). (B): The number of the injected UC MSCs per area (mm^2). Bar charts present mean ± standard deviation; statistically significant at $p < .05$. Abbreviations: DAPI, 4′,6-diamidino-2-phenylindole; UC MSCs, umbilical cord derived mesenchymal stem cells.

https://doi.org/10.1371/journal.pone.0235239.g006

collagen organization in the UC MSCs group than in the saline group at four weeks; 3) the area of cartilage-related GAG was significantly less in the UC MSCs group than in the saline group at four weeks and heterotopic ossification was not observed at any groups; 4) the ultimate failure load was significantly greater in the UC MSCs group than that in the saline group at two and four weeks. Especially, the ultimate failure load in the UC MSCs group at four weeks was comparable with that of the control group; and 5) intratendinously injected UC MSCs disappeared over time, and 5.29% of those at three hours were retained in the tendon defect at four weeks after injection. Taken together, these results showed that intratendinous injection of UC MSCs would affect regeneration of the FTD with the formation of collagen matrix while suppressing heterotopic matrix changes, and thus improved the ultimate failure

load comparable to normal tendon at 4 weeks in a rat model suggesting potentials of UC MSCs injection for the treatment of the FTD without surgical repair.

Clinically, rotator cuff disease is known to progress from tendinopathy to the PTD, and then to the FTD [28]. The FTD has been reported to increase in size over time [39]. Progression of rotator cuff disease does not only mean an increase of the size of the FTD, but also the deterioration of tendon structure and quality, and degeneration of rotator cuff muscles [40, 41]. Therefore, it would be crucial to prevent or halt, or should be better to reverse its progression though the regeneration of the FTD. Several researchers have shown regenerative potentials of MSCs in patellar tendon defect model, Achilles tendon defect and incision models, superficial digital flexor tendon core lesion model and Achilles tendinopathy model [42, 43]. For surgical repair model of rotator cuff tear, several studies demonstrated that MSCs from BM, AD, and tendon implanted with scaffold have shown promising results in repair and defect models [44, 45]. However, there were few studies that delivered MSCs via injection for the investigation of regeneration of rotator cuff tendon in animal model; one study injected UCB MSCs with hyaluronic acid into subscapularis defect in a rabbit model, and one injected AD MSCs in phosphate buffered saline into tendinopathy lesion of SST in a rat model [13, 46]. In this study, we injected human UC MSCs adjacent to the FTD in a rat model without any carrier which could be feasibly translated in daily practice. In this study, we observed UC MSCs could prevent rotator cuff tear from progression to worst over time by preventing the tear size from increasing, whereas the defect size increased in the saline group. Furthermore, tendon thickness, inflammation, defect size, swelling/redness and connection surrounding tissue and slidability also improved in the UC MSCs group compared to the saline group. These results demonstrated healing potentials of injected UC MSCs without carrier for the treatment of the FTD which is consistent with that of the previous study.

The main cause of unsuccessful tendon healing is the formation of a fibrovascular scar tissue after injury [47]. Scar tissue has decreased and disorganized collagen matrix with reduced collagen 1/3 ratio [48], as well as increased vascularity and angled and rounded nuclei of fibroblasts [49]. Previously, there are several studies trying to return the degenerated tendon structure to its previous normal tendon structure using MSC treatments [50, 51]. BM MSCs improved general tendon structure such as fiber structure, arrangement, in Achilles tendon rupture rat model at 30 days [51] and AD MSCs improved matrix organization in Achilles tendon defect model at 3 and 4.5 weeks [50]. Nonetheless, these results did not clearly show that BM and AD MSCs reduced scar tissue formation, because histological criteria for the scar tissue has not been clear [50, 51]. In this study, we established a histological evaluation system that encompassed various currently accepted methods that could define scar tissue in tendon. General tendon structure including collagen matrix, cell, vascularity, hyalinization, integration and inflammation was evaluated by H&E staining and light microscopy, and collagen fiber organization and coherency were analyzed by PSR staining and polarized light microscopy. Heterotopic matrix changes were evaluated by Saf-O staining using light microscopy. Furthermore, we used computerized image analysis to quantification of changes of tendon structure. With this system, we found UC MSCs could improve tendon structure suppressing abnormal scar tissue formation and the regenerated tendon structure was comparable to normal tendon tissue.

Cartilage-related GAG rich area or hyalinization, calcific tendinopathy and heterotopic ossification has been commonly reported in patients with tendinopathy and tendon rupture [52]. In addition, chondrocyte phenotype and ectopic bone formation has been frequently described in surgically induced defect models and collagenase-induced tendinopathy models [53, 54]. Furthermore, BM MSCs application for tendon regeneration evoked heterotopic ossification both in defect and tendinopathy models [15, 55]. The presence of heterotopic ossification in tendon worsens the clinical manifestations of tendon injury [56], may lead to

increase rupture rates and recovery time [57], and cause a higher frequency of post-operative complications such as shoulder pain [58]. Therefore, it is crucial to suppress heterotopic ossification for the treatment of tendon injury with MSC implantation. With respect to the occurrence of heterotopic ossification, current evidences raise concerns over the use of BM MSCs for tendon regeneration because they were prone to osteogenic differentiation with a higher chance of heterotopic ossification up to 55% of cases in experimental studies. However, in this study, UC MSCs reduced heterotopic cartilage-related GAG formation by 73% of saline treated tendons at four weeks and did not cause any heterotopic ossification. Although it had not been studied how to inhibit heterotopic cartilage or bone formation by UC MSCs, these results demonstrated that UC MSCs could suppress heterotopic matrix changes and ossification suggesting that UC MSCs is a safer option than BM MSCs for tendon regeneration.

Several studies showed that MSCs application improved some of biomechanical properties of surgically repaired and collagenase-induced tendinopathy models [13, 42]. However, the enhanced properties provided with MSCs may not last longer time or some parameters such as ultimate stress did not improve with application of MSCs [13, 42, 50]. In this study, UC MSCs injection significantly increased the ultimate failure load and ultimate stress at two and four weeks, and also improved stiffness at two weeks compared to the saline injection. Especially the ultimate failure load increased by 88% to a level comparable to the normal tendon at four weeks. Furthermore, the ultimate stress in the UC MSCs group were significantly higher by 1.4-fold both at two and four weeks after injection than that in the saline group. These improved biomechanical results were corroborated by the improved histologic results in this study. Biomechanical properties of tendon are derived from well aligned and organized collagen fibers of tendon [50, 59]. Thus, we though that UC MSCs could promote the recovery of the tendon structure, then the recovered tendon structure could induce the functional recovery of the rotator cuff.

Although there were tendon structural and functional improvements until four weeks after UC MSCs injection, most of the injected UC MSCs disappeared at the defected tendon over time. Previous studies have demonstrated that positive effects of MSCs come from the paracrine mechanism by secretion of cytokines and growth factors [60] and MSC could regulate local environment of injured site by modulating macrophage recruitment and polarization to M2 phenotype [10, 61]. For these reasons, even though most of the injected UC MSCs faded away over time, the local environment modulated by UC MSCs still had a benefit effect on recovery of structure of injured tendon. However, more study is needed to demonstrate the cellular mechanism in which UC MSC improve the regeneration of injured tendon.

There are several limitations in this study. First, an acute tendon defect model which might not reflect chronic tendon degeneration, one of the most important causes of rotator cuff tear, was used. However, the total degeneration scores in the saline group at two and four weeks were similar to those in patients with a full-thickness rotator cuff tear. Second, evaluation period of four weeks would be short for clearer assessment of effects of UC MSCs for rotator cuff tendon regeneration as lots of parameters in the study were expected to further improve in a longer follow-up period.

This study demonstrated that UC MSCs regenerated the FTD with tendon tissue similar properties to the normal tendon in terms of macroscopic, histological and biomechanical characteristics in a rat model through directly inject to the injury site without any carrier materials.

Supporting information

S1 Table. This is the modified macroscopic evaluation system table.
(DOCX)

S2 Table. This is the macroscopic evaluation results of tendon regeneration.
(DOCX)

Author Contributions

Conceptualization: Ji-Hye Yea, Chris Hyunchul Jo.

Data curation: Ji-Hye Yea, Tae Soo Bae.

Formal analysis: Ji-Hye Yea.

Funding acquisition: Chris Hyunchul Jo.

Investigation: Ji-Hye Yea.

Methodology: Ji-Hye Yea.

Project administration: Chris Hyunchul Jo.

Resources: Ji-Hye Yea, InJa Kim, Gayoung Sym, Jin-Kyung Park, Ah-Young Lee, Byeong Chan Cho, Tae Soo Bae, Byoung Jae Kim.

Supervision: Chris Hyunchul Jo.

Visualization: Ji-Hye Yea.

Writing – original draft: Ji-Hye Yea.

Writing – review & editing: Tae Soo Bae, Chris Hyunchul Jo.

References

1. Abat F, Alfredson H, Cucchiarini M, Madry H, Marmotti A, Mouton C, et al. Current trends in tendinopathy: consensus of the ESSKA basic science committee. Part I: biology, biomechanics, anatomy and an exercise-based approach. J Exp Orthop. 2017; 4(1):1–18. https://doi.org/10.1186/s40634-017-0092-6 PMID: 28560707

2. Hermans J, Luime JJ, Meuffels DE, Reijman M, Simel DL, Bierma-Zeinstra SMA. Does This Patient With Shoulder Pain Have Rotator Cuff Disease? The Rational Clinical Examination Systematic Review. Jama-J Am Med Assoc. 2013; 310(8):837–47. https://doi.org/10.1001/jama.2013.276187 PMID: 23982370

3. Schneider M, Angele P, Jarvinen TAH, Docheva D. Rescue plan for Achilles: Therapeutics steering the fate and functions of stem cells in tendon wound healing. Adv Drug Deliv Rev. 2018; 129:352–75. https://doi.org/10.1016/j.addr.2017.12.016 PMID: 29278683

4. Narayanan G, Nair LS, Laurencin CT. Regenerative Engineering of the Rotator Cuff of the Shoulder. Acs Biomater Sci Eng. 2018; 4(3):751–86.

5. Karasuyama M, Gotoh M, Tahara K, Kawakami J, Madokoro K, Nagamatsu T, et al. Clinical results of conservative management in patients with full-thickness rotator cuff tear: a meta-analysis. Clinics in Shoulder and Elbow. 2020; 23(2):86–93.

6. Merolla G, Paladini P, Saporito M, Porcellini G. Conservative management of rotator cuff tears: literature review and proposal for a prognostic. Prediction Score. Muscles Ligaments Tendons J. 2011; 1 (1):12–9. PMID: 23738239

7. van der Windt DA, Koes BW, Boeke AJ, Deville W, De Jong BA, Bouter LM. Shoulder disorders in general practice: prognostic indicators of outcome. Br J Gen Pract. 1996; 46(410):519–23. PMID: 8917870

8. Abraham AC, Shah SA, Thomopoulos S. Targeting Inflammation in Rotator Cuff Tendon Degeneration and Repair. Tech Shoulder Elbow. 2017; 18(3):84–90. https://doi.org/10.1097/BTE.0000000000000124 PMID: 28947893

9. Uthoff H, Spenner A, Reckelkamm W, Ahrens B, Wolk G, Hackler R, et al. Critical role of preconceptional immunization for protective and nonpathological specific immunity in murine neonates. J Immunol. 2003; 171(7):3485–92. https://doi.org/10.4049/jimmunol.171.7.3485 PMID: 14500644

10. Bianco ST, Moser HL, Galatz LM, Huang AH. Biologics and stem cell-based therapies for rotator cuff repair. Ann N Y Acad Sci. 2018; 1442(1):35–47. https://doi.org/10.1111/nyas.13918 PMID: 30008172

11. De Miguel MP, Fuentes-Julian S, Blazquez-Martinez A, Pascual CY, Aller MA, Arias J, et al. Immuno-suppressive Properties of Mesenchymal Stem Cells: Advances and Applications. Curr Mol Med. 2012; 12(5):574–91. https://doi.org/10.2174/156652412800619950 PMID: 22515979

12. Degen RM, Carbone A, Carballo C, Zong JC, Chen T, Lebaschi A, et al. The Effect of Purified Human Bone Marrow-Derived Mesenchymal Stem Cells on Rotator Cuff Tendon Healing in an Athymic Rat. Arthroscopy. 2016; 32(12):2435–43. https://doi.org/10.1016/j.arthro.2016.04.019 PMID: 27282111

13. Chen HS, Su YT, Chan TM, Su YJ, Syu WS, Harn HJ, et al. Human adipose-derived stem cells acceler-ate the restoration of tensile strength of tendon and alleviate the progression of rotator cuff injury in a rat model. Cell Transplant. 2015; 24(3):509–20. https://doi.org/10.3727/096368915X686968 PMID: 25654771

14. Troyer DL, Weiss ML. Concise review: Wharton's jelly-derived cells are a primitive stromal cell popula-tion. Stem Cells. 2008; 26(3):591–9. https://doi.org/10.1634/stemcells.2007-0439 PMID: 18065397

15. Hsieh CF, Alberton P, Loffredo-Verde E, Volkmer E, Pietschmann M, Muller P, et al. Scaffold-free Scleraxis-programmed tendon progenitors aid in significantly enhanced repair of full-size Achilles ten-don rupture. Nanomedicine (Lond). 2016; 11(9):1153–67. https://doi.org/10.2217/nnm.16.34 PMID: 27074105

16. Beeravolu N, Khan I, McKee C, Dinda S, Thibodeau B, Wilson G, et al. Isolation and comparative analy-sis of potential stem/progenitor cells from different regions of human umbilical cord. Stem Cell Res. 2016; 16(3):696–711. https://doi.org/10.1016/j.scr.2016.04.010 PMID: 27107345

17. Conconi MT, Burra P, Di Liddo R, Calore C, Turetta M, Bellini S, et al. CD105(+) cells from Wharton's jelly show in vitro and in vivo myogenic differentiative potential. Int J Mol Med. 2006; 18(6):1089–96. PMID: 17089012

18. Wu KH, Zhou B, Lu SH, Feng B, Yang SG, Du WT, et al. In vitro and in vivo differentiation of human umbilical cord derived stem cells into endothelial cells. J Cell Biochem. 2007; 100(3):608–16. https://doi.org/10.1002/jcb.21078 PMID: 16960877

19. Li MR, Luan FX, Zhao YL, Hao HJ, Liu JJ, Dong L, et al. Mesenchymal stem cell-conditioned medium accelerates wound healing with fewer scars. International Wound Journal. 2017; 14(1):64–73. https://doi.org/10.1111/iwj.12551 PMID: 26635066

20. Emrani H, Davies JE Umbilical cord perivascular cells: a mesenchymal cell source for treatment of ten-don injuries. JTOTE, Journal RM. 2011; 4(1).

21. Kwon DR, Park GY, Moon YS, Lee SC. Therapeutic Effects of Umbilical Cord Blood-Derived Mesen-chymal Stem Cells Combined with Polydeoxyribonucleotides on Full-Thickness Rotator Cuff Tendon Tear in a Rabbit Model. Cell Transplant. 2018; 27(11):1613–22. https://doi.org/10.1177/0963689718799040 PMID: 30270645

22. Kwon DR, Park GY, Lee SC. Treatment of Full-Thickness Rotator Cuff Tendon Tear Using Umbilical Cord Blood-Derived Mesenchymal Stem Cells and Polydeoxyribonucleotides in a Rabbit Model. Stem Cells Int. 2018; 2018:7146384. https://doi.org/10.1155/2018/7146384 PMID: 29861743

23. Jo CH, Kim OS, Park EY, Kim BJ, Lee JH, Kang SB, et al. Fetal mesenchymal stem cells derived from human umbilical cord sustain primitive characteristics during extensive expansion. Cell Tissue Res. 2008; 334(3):423–33. https://doi.org/10.1007/s00441-008-0696-3 PMID: 18941782

24. Yea J-H, Park J-K, Kim IJ, Sym G, Bae T-S, Jo CH. Regeneration of a full-thickness defect of rotator cuff tendon with freshly thawed umbilical cord-derived mesenchymal stem cells in a rat model. Stem Cell Research & Therapy. 2020; 11(1):1–13. https://doi.org/10.1186/s13287-020-01906-1 PMID: 32894193

25. Carpenter JE, Thomopoulos S, Flanagan CL, DeBano CM, Soslowsky LJ. Rotator cuff defect healing: a biomechanical and histologic analysis in an animal model. J Shoulder Elbow Surg. 1998; 7(6):599–605. https://doi.org/10.1016/s1058-2746(98)90007-6 PMID: 9883420

26. Choi HR, Kondo S, Hirose K, Ishiguro N, Hasegawa Y, Iwata H. Expression and enzymatic activity of MMP-2 during healing process of the acute supraspinatus tendon tear in rabbits. J Orthop Res. 2002; 20(5):927–33. https://doi.org/10.1016/S0736-0266(02)00016-5 PMID: 12382955

27. Stoll C, John T, Conrad C, Lohan A, Hondke S, Ertel W, et al. Healing parameters in a rabbit partial ten-don defect following tenocyte/biomaterial implantation. Biomaterials. 2011; 32(21):4806–15. https://doi.org/10.1016/j.biomaterials.2011.03.026 PMID: 21474176

28. Jo CH, Shin WH, Park JW, Shin JS, Kim JE. Degree of tendon degeneration and stage of rotator cuff disease. Knee Surg Sport Tr A. 2017; 25(7):2100–8. https://doi.org/10.1007/s00167-016-4376-7 PMID: 27896393

29. Chen L, Liu JP, Tang KL, Wang Q, Wang GD, Cai XH, et al. Tendon derived stem cells promote plate-let-rich plasma healing in collagenase-induced rat achilles tendinopathy. Cell Physiol Biochem. 2014; 34(6):2153–68. https://doi.org/10.1159/000369659 PMID: 25562162

30. Kraus TM, Imhoff FB, Reinert J, Wexel G, Wolf A, Hirsch D, et al. Stem cells and bFGF in tendon healing: Effects of lentiviral gene transfer and long-term follow-up in a rat Achilles tendon defect model. Bmc Musculoskel Dis. 2016; 17(148):1–7.

31. Fernandez-Sarmiento JA, Dominguez JM, Granados MM, Morgaz J, Navarrete R, Carrillo JM, et al. Histological study of the influence of plasma rich in growth factors (PRGF) on the healing of divided Achilles tendons in sheep. J Bone Joint Surg Am. 2013; 95(3):246–55. https://doi.org/10.2106/JBJS.K. 01659 PMID: 23389788

32. Zhao S, Zhao JW, Dong SK, Huangfu XQ, Bin L, Yang HL, et al. Biological augmentation of rotator cuff repair using bFGF-loaded electrospun poly(lactide-co-glycolide) fibrous membranes. Int J Nanomed. 2014; 9:2373–85. https://doi.org/10.2147/IJN.S59536 PMID: 24868155

33. Galatz LM, Charlton N, Das R, Kim HM, Havlioglu N, Thomopoulos S. Complete removal of load is detrimental to rotator cuff healing. J Shoulder Elb Surg. 2009; 18(5):669–75. https://doi.org/10.1016/j.jse. 2009.02.016 PMID: 19427237

34. Beck J, Evans D, Tonino PM, Yong S, Callaci JJ. The biomechanical and histologic effects of platelet-rich plasma on rat rotator cuff repairs. The American journal of sports medicine. 2012; 40(9):2037–44. https://doi.org/10.1177/0363546512453300 PMID: 22822177

35. Galatz L, Silva M, Rothermich S, Zaegel M, Havlioglu N, Thomopoulos S. Nicotine delays tendon-to-bone healing in a rat shoulder model. JBJS. 2006; 88(9):2027–34.

36. Yea J-H, Bae TS, Kim BJ, Cho YW, Jo CH. Regeneration of the rotator cuff tendon-to-bone interface using umbilical cord-derived mesenchymal stem cells and gradient extracellular matrix scaffolds from adipose tissue in a rat model. Acta Biomater. 2020; 114:104–16. https://doi.org/10.1016/j.actbio.2020. 07.020 PMID: 32682057

37. Li SY, Gao Y, Tokuyama T, Yamamoto J, Yokota N, Yamamoto S, et al. Genetically engineered neural stem cells migrate and suppress glioma cell growth at distant intracranial sites. Cancer Letters. 2007; 251(2):220–7. https://doi.org/10.1016/j.canlet.2006.11.024 PMID: 17196326

38. Kang ES, Ha KY, Kim YH. Fate of transplanted bone marrow derived mesenchymal stem cells following spinal cord injury in rats by transplantation routes. J Korean Med Sci. 2012; 27(6):586–93. https://doi. org/10.3346/jkms.2012.27.6.586 PMID: 22690088

39. Yamaguchi K, Tetro AM, Blam O, Evanoff BA, Teefey SA, Middleton WD. Natural history of asymptomatic rotator cuff tears: a longitudinal analysis of asymptomatic tears detected sonographically. J Shoulder Elbow Surg. 2001; 10(3):199–203. https://doi.org/10.1067/mse.2001.113086 PMID: 11408898

40. Hebert-Davies J, Teefey SA, Steger-May K, Chamberlain AM, Middleton W, Robinson K, et al. Progression of Fatty Muscle Degeneration in Atraumatic Rotator Cuff Tears. J Bone Joint Surg Am. 2017; 99 (10):832–9. https://doi.org/10.2106/JBJS.16.00030 PMID: 28509823

41. Tashjian RZ. Epidemiology, natural history, and indications for treatment of rotator cuff tears. Clin Sports Med. 2012; 31(4):589–604. https://doi.org/10.1016/j.csm.2012.07.001 PMID: 23040548

42. Lee SY, Kwon B, Lee K, Son YH, Chung SG. Therapeutic Mechanisms of Human Adipose-Derived Mesenchymal Stem Cells in a Rat Tendon Injury Model. Am J Sports Med. 2017; 45(6):1429–39. https://doi.org/10.1177/0363546517689874 PMID: 28291954

43. Machova Urdzikova L, Sedlacek R, Suchy T, Amemori T, Ruzicka J, Lesny P, et al. Human multipotent mesenchymal stem cells improve healing after collagenase tendon injury in the rat. Biomed Eng Online. 2014; 13(42):1–15. https://doi.org/10.1186/1475-925X-13-42 PMID: 24712305

44. Gulotta LV, Kovacevic D, Ehteshami JR, Dagher E, Packer JD, Rodeo SA. Application of bone marrow-derived mesenchymal stem cells in a rotator cuff repair model. Am J Sports Med. 2009; 37(11):2126–33. https://doi.org/10.1177/0363546509339582 PMID: 19684297

45. Killian ML, Lim CT, Thomopoulos S, Charlton N, Kim HM, Galatz LM. The effect of unloading on gene expression of healthy and injured rotator cuffs. J Orthop Res. 2013; 31(8):1240–8. https://doi.org/10. 1002/jor.22345 PMID: 23508698

46. Park GY, Kwon DR, Lee SC. Regeneration of Full-Thickness Rotator Cuff Tendon Tear After Ultrasound-Guided Injection With Umbilical Cord Blood-Derived Mesenchymal Stem Cells in a Rabbit Model. Stem Cells Transl Med. 2015; 4(11):1344–51. https://doi.org/10.5966/sctm.2015-0040 PMID: 26371340

47. Yang G, Rothrauff BB, Tuan RS. Tendon and ligament regeneration and repair: clinical relevance and developmental paradigm. Birth Defects Res C Embryo Today. 2013; 99(3):203–22. https://doi.org/10. 1002/bdrc.21041 PMID: 24078497

48. Lapiere CM, Nusgens B, Pierard GE. Interaction between collagen type I and type III in conditioning bundles organization. Connect Tissue Res. 1977; 5(1):21–9. https://doi.org/10.3109/03008207709152608 PMID: 141359

49. Pittenger MF, Mackay AM, Beck SC, Jaiswal RK, Douglas R, Mosca JD, et al. Multilineage potential of adult human mesenchymal stem cells. Science. 1999; 284(5411):143–7.

50. Norelli JB, Plaza DP, Stal DN, Varghese AM, Liang H, Grande DA. Tenogenically differentiated adipose-derived stem cells are effective in Achilles tendon repair in vivo. J Tissue Eng. 2018; 9(1):1–20. https://doi.org/10.1177/2041731418811183 PMID: 30542597

51. Yuksel S, Gulec MA, Gultekin MZ, Adanir O, Caglar A, Beytemur O, et al. Comparison of the early period effects of bone marrow-derived mesenchymal stem cells and platelet-rich plasma on the Achilles tendon ruptures in rats. Connect Tissue Res. 2016; 57(5):360–73. https://doi.org/10.1080/03008207.2016.1189909 PMID: 27191749

52. Corps AN, Robinson AH, Movin T, Costa ML, Hazleman BL, Riley GP. Increased expression of aggrecan and biglycan mRNA in Achilles tendinopathy. Rheumatology (Oxford). 2006; 45(3):291–4. https://doi.org/10.1093/rheumatology/kei152 PMID: 16219640

53. Lui PP, Fu SC, Chan LS, Hung LK, Chan KM. Chondrocyte phenotype and ectopic ossification in collagenase-induced tendon degeneration. J Histochem Cytochem. 2009; 57(2):91–100. https://doi.org/10.1369/jhc.2008.952143 PMID: 18824634

54. Lui PP, Cheuk YC, Lee YW, Chan KM. Ectopic chondro-ossification and erroneous extracellular matrix deposition in a tendon window injury model. J Orthop Res. 2012; 30(1):37–46. https://doi.org/10.1002/jor.21495 PMID: 21761446

55. Awad HA, Boivin GP, Dressler MR, Smith FN, Young RG, Butler DL. Repair of patellar tendon injuries using a cell-collagen composite. J Orthop Res. 2003; 21(3):420–31. https://doi.org/10.1016/S0736-0266(02)00163-8 PMID: 12706014

56. Maffulli N, Wong J, Almekinders LC. Types and epidemiology of tendinopathy. Clin Sports Med. 2003; 22(4):675–92. https://doi.org/10.1016/s0278-5919(03)00004-8 PMID: 14560540

57. Hashimoto T, Nobuhara K, Hamada T. Pathologic evidence of degeneration as a primary cause of rotator cuff tear. Clin Orthop Relat R. 2003(415):111–20. https://doi.org/10.1097/01.blo.0000092974.12414.22 PMID: 14612637

58. Aina R, Cardinal E, Bureau NJ, Aubin B, Brassard P. Calcific shoulder tendinitis: Treatment with modified US-guided fine-needle technique. Radiology. 2001; 221(2):455–61. https://doi.org/10.1148/radiol.2212000830 PMID: 11687690

59. Gimbel JA, Van Kleunen JP, Mehta S, Perry SM, Williams GR, Soslowsky LJ. Supraspinatus tendon organizational and mechanical properties in a chronic rotator cuff tear animal model. J Biomech. 2004; 37(5):739–49. https://doi.org/10.1016/j.jbiomech.2003.09.019 PMID: 15047003

60. Zhang B, Luo Q, Halim A, Ju Y, Morita Y, Song G. Directed Differentiation and Paracrine Mechanisms of Mesenchymal Stem Cells: Potential Implications for Tendon Repair and Regeneration. Curr Stem Cell Res Ther. 2017; 12(6):447–54.

61. El Omar R, Beroud J, Stoltz JF, Menu P, Velot E, Decot V. Umbilical cord mesenchymal stem cells: the new gold standard for mesenchymal stem cell-based therapies? Tissue Eng Part B Rev. 2014; 20(5):523–44. https://doi.org/10.1089/ten.TEB.2013.0664 PMID: 24552279